AMERICAN SOCIETY FOR MICROBIOLOGY | mBio®

RESEARCH ARTICLE

Investigation of the Genetics and Biochemistry of Roseobacticide Production in the *Roseobacter* Clade Bacterium *Phaeobacter inhibens*

Rurun Wang,[a] Étienne Gallant,[a] Mohammad R. Seyedsayamdost[a,b]

Department of Chemistry[a] and Department of Molecular Biology,[b] Princeton University, Princeton, New Jersey, USA

ABSTRACT ***Roseobacter*** **clade bacteria are abundant in surface waters and are among the most metabolically diverse and ecologically significant species. This group includes opportunistic symbionts that associate with micro- and macroalgae. We have proposed that one representative member, *Phaeobacter inhibens*, engages in a dynamic symbiosis with the microalga *Emiliania huxleyi*. In one phase, mutualistically beneficial molecules are exchanged, including the *Roseobacter*-produced antibiotic tropodithietic acid (TDA), which is thought to protect the symbiotic interaction. In an alternative parasitic phase, triggered by algal senescence, the bacteria produce potent algaecides, the roseobacticides, which kill the algal host. Here, we employed genetic and biochemical screens to identify the roseobacticide biosynthetic gene cluster. By using a transposon mutagenesis approach, we found that genes required for TDA synthesis—the *tda* operon and *paa* catabolon—are also necessary for roseobacticide production. Thus, in contrast to the one-cluster–one-compound paradigm, the *tda* gene cluster can generate two sets of molecules with distinct structures and bioactivities. We further show that roseobacticide production is quorum sensing regulated via an *N*-acyl homoserine lactone signal (3-OH–C_{10}-HSL). To ensure tight regulation of algaecide production, and thus of a lifestyle switch from mutualism to parasitism, roseobacticide biosynthesis necessitates the presence of both an algal senescence molecule and a quorum sensing signal.**

IMPORTANCE **Marine *Roseobacter* species are abundant in the oceans and engage in symbiotic interactions with microscopic algae. One member, *P. inhibens*, produces the antibiotic TDA and a growth hormone thought to protect and promote algal growth. However, in the presence of molecules released by senescing algae, the bacteria produce potent algaecides, the roseobacticides, which kill the host. We examined the regulatory networks and biosynthetic genes required for roseobacticide production. We found that *P. inhibens* uses largely the same set of genes for production of both TDA and roseobacticides, thus providing a rare case in which one gene cluster synthesizes two structurally and functionally distinct molecules. Moreover, we found roseobacticide production to be regulated by quorum sensing. Thus, two small molecules, the algal metabolite and the quorum-sensing signal, ensure tight control in the production of roseobacticides. These results highlight the role of small molecules in regulating microbial symbioses.**

Received 5 December 2015 **Accepted** 17 February 2016 **Published** 22 March 2016

Citation Wang R, Gallant É, Seyedsayamdost MR. 2016. Investigation of the genetics and biochemistry of roseobacticide production in the *Roseobacter* clade bacterium *Phaeobacter inhibens*. mBio 7(2):e02118-15. doi:10.1128/mBio.02118-15.

Editor Nicole Dubilier, Max Planck Institute for Marine Microbiology

Address correspondence to Mohammad R. Seyedsayamdost, mrseyed@princeton.edu.

The wealth of bacterial genome sequences has deeply impacted our ability to connect an isolated secondary metabolite to its biosynthetic gene cluster. With recent advances in bioinformatics, the first step in this process typically involves a computational approach (1). However, in the case of small molecules that belong to a new chemotype and do not represent the typical structural classes, such as nonribosomal peptides (NRP) or polyketides (PK), this process is much more challenging. Identifying the biosynthetic gene clusters of these types of molecules requires bacterial genetic methods with screens tailored toward the biological or chemical properties of the molecule of interest. Roseobacticides, a family of tropolactone natural products, represent an example of this category of molecules (2). They are not derived from NRP/PK biosynthetic pathways, contain a unique chemical scaffold, and are synthesized by an as-yet-unknown biosynthetic pathway and gene cluster.

Roseobacticides are produced by *Phaeobacter inhibens*, a member of the *Roseobacter* clade of alphaproteobacteria, which are abundant in the oceans, especially in coastal regions during algal blooms (3, 4). Aside from their abundance, *Roseobacter* are known for their ability to colonize biotic and abiotic surfaces and interact with microalgae, macroalgae, and other eukaryotes (5–7). Numerous studies have demonstrated beneficial roles for bacterial colonization of algal surfaces, suggesting a mutualistic association (8–10). On the basis of recent results, we have proposed that *P. inhibens* engages in a biphasic symbiosis with microalgae, such as *Emiliania huxleyi*, with each phase of the symbiosis characterized by a set of small molecules (Fig. 1) (2, 11). In the mutualistic phase, the algae provide dimethylsulfoniopropionate (DMSP), which the bacteria move toward via chemotaxis and use as a source of carbon and sulfur (12–14). In return, the bacteria generate phenylacetic acid, which has been shown to serve as a growth

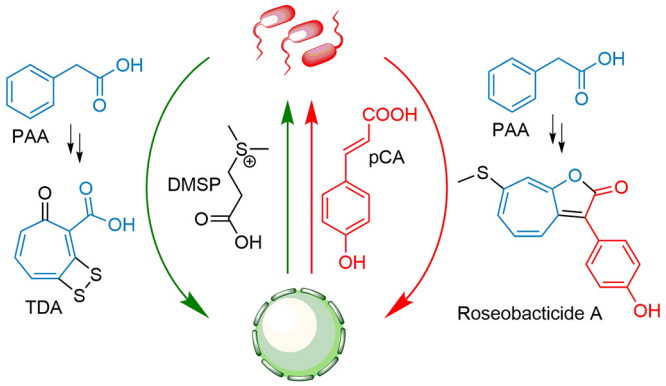

FIG 1 Model for algal-bacterial symbiosis involving *P. inhibens* and *E. huxleyi*. The symbiosis comprises two modes, a mutualistic phase (green arrows) and a parasitic phase (red arrows) (2). In the mutualistic phase, phenylacetic acid (PAA) provides a precursor for TDA, and both metabolites serve as beneficial molecules to the algae, which provide the bacteria with food in the form of DMSP. In the parasitic phase, the senescing algal host releases pCA. The bacteria respond by combining fragments of DMSP, PAA, and pCA to synthesize the algaecide roseobacticide A (23).

promoter in some algae, and an antibiotic, tropodithietic acid (TDA), to which has been attributed general aquacultural benefits, including protection of microalgae and other eukaryotes from unwanted marine pathogens (15–19). When the algae senesce, however, the interaction changes. Under these conditions, the host produces *p*-coumaric acid (pCA), which triggers production of potent bacterial algaecides, the roseobacticides (2). These compounds kill the algal host with nanomolar to micromolar efficiency in laboratory experiments. The abundance of *Roseobacter* observed at the conclusion of algal blooms and the detection of bacterial algaecidal activity in other systems are consistent with this mutualist-to-parasite switch model (20–22). Roseobacticides are cryptic metabolites: their production is tightly regulated, that is, they are not observed under a number of conditions lacking pCA and have only been observed in the presence of phenylpropanoid inducers, such as pCA or sinapic acid (2, 11).

Aside from their important biological activity, roseobacticides constitute a new structural class of natural products and as such their biosynthesis is of great interest, as it promises to uncover new enzymatic transformations. Our recent examination of the biosynthetic pathway of roseobacticides by isotope feeding experiments revealed that phenylacetic acid, phenylglyoxylic acid, and Cys—which is derived from DMSP in a natural setting—are utilized as roseobacticide precursors. Not only did these studies provide a biosynthetic model for the roseobacticides, they also demonstrated a remarkable metabolic economy in the conversion of molecules involved in the mutualistic phase (DMSP and phenylacetic acid) into toxins in the parasitic phase (Fig. 1).

Much like roseobacticides, the related tropone-bearing TDA is also structurally unusual (Fig. 1) (24–26). While tropone-containing metabolites have been shown to be produced in a polyketide synthase-dependent manner in fungi (27), TDA biosynthesis in *P. inhibens* occurs by a different strategy (15, 28, 29). The biochemical pathway for TDA production has been investigated for over 20 years, but a consensus pathway has yet to be determined. The regulatory and biosynthetic genes have been identified through a comprehensive transposon mutagenesis screen, which utilized the potent antibacterial activity of TDA against *Vibrio anguillarum* to search for mutants that no longer exhibited growth-inhibitory effects (28). This approach identified the *tda* operon, as well as a number of other biosynthetic loci that in a concerted fashion give rise to TDA. These genes code for small biosynthetic enzymes, most without recognizable signature motifs, and as such, identifying them by bioinformatic means would be exceedingly difficult. Using a similar approach, we hoped to answer questions regarding the regulation and biosynthesis of roseobacticides. Here, we have employed random transposon mutagenesis along with a high-throughput fluorescence assay to identify genes involved in roseobacticide synthesis. We report that roseobacticide production is regulated via quorum sensing (QS) and that it shares a late common intermediate with the TDA biosynthetic pathway, as these two processes share a number of enzymes. Thus, the *tda* locus gives rise not only to TDA but also to roseobacticides, providing an unusual case in which one gene cluster is responsible for the synthesis of two structurally and functionally distinct secondary metabolites.

RESULTS AND DISCUSSION

Choice of random mutagenesis and assay systems. To identify the biosynthetic genes required for roseobacticide production, we initiated a transposon mutagenesis study, in which we planned to generate a library of mutants and identify those that do not produce roseobacticides in the presence of pCA. Roseobacticides do not harbor antibacterial activity that can be carried out in a high-throughput fashion. While they kill *E. huxleyi* (with a half-maximal inhibitory concentration of 0.1 μM in the case of roseobacticide B), carrying out this assay with thousands of mutants proved impractical.

Given that the bioactivity of roseobacticides is difficult to test in a high-throughput format, we turned our attention to their chemical properties. Roseobacticides display absorption features with a λ_{max} of 430 nm and extinction coefficient (ε) of 6,000 M^{-1} cm^{-1} (see Fig. S1 in the supplemental material). These properties, however, were not sufficient to discern the presence of roseobacticides in cultures, due to interference from the medium of choice, which gave background absorption at 430 nm. Fluorescence spectroscopy, however, provided a viable alternative (Fig. 2). The fluorescence emission spectrum of *P. inhibens* cultures showed an emission wavelength (λ_{em}) of 510 nm (excitation wavelength [λ_{ex}] of 430 nm) only in the presence of the inducer sinapic acid. This was not due to the yeast extract-tryptone-sea salt (YTSS) medium or sinapic acid and correlated with roseobacticide production (Fig. 2). Thus, fluorescence emission coupled with the EZ-Tn*5* transposome system offered an efficient mutagenesis and assay system. We optimized a workflow in which a library of Tn*5* mutants was generated on agar and subsequently arrayed into 96-well plates. Assay plates containing the inducer sinapic acid were then inoculated with the arrayed library plate, grown for 3 days, and then analyzed by fluorescence spectroscopy. The use of black-walled, clear-bottom 96-well plates allowed us to determine the optical density at 600 nm (OD_{600}) and fluorescence emission spectra for each mutant, thus removing from our analysis mutants that failed to grow while also enabling normalization for cell density. Mutants were defined as those that displayed <5% of the λ_{em} intensity of wild-type (wt) cells with sinapic acid or yielded entirely different emission spectra.

Transposon screen and validation. *P. inhibens* contains 3,960 open reading frames. We generated an array library of ~8,000

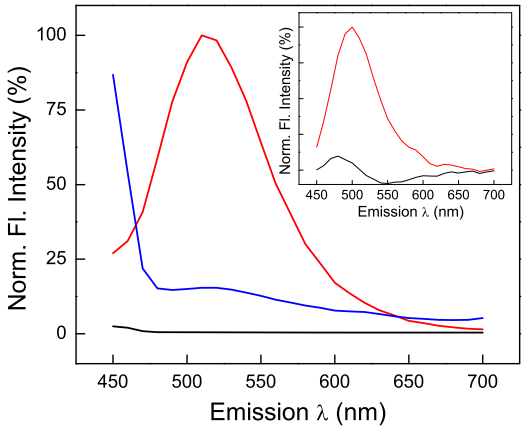

FIG 2 Monitoring roseobacticide production by fluorescence spectroscopy. Samples were excited at the absorbance maximum of roseobacticides (430 nm), and emission was monitored between 450 and 700 nm. Shown are emission spectra for YTSS medium with sinapic acid (black trace), cultures of *P. inhibens* in YTSS in the absence of inducer sinapic acid (blue trace), and cultures of *P. inhibens* in YTSS in the presence of sinapic acid (red trace). (Inset) Fluorescence emission spectra of wt *P. inhibens* (red trace) and a *P. inhibens* Tn mutant (Tn*5*::PGA1_262p00840) that is deficient in roseobacticide synthesis. Both were grown in the presence of 1 mM sinapic acid in a 96-well assay plate. The emission trace of wt *P. inhibens* grown in the absence of sinapic acid has been subtracted from both spectra to remove fluorescence emission properties not associated with roseobacticide production (normalized fluorescence [Norm. Fl.] intensity).

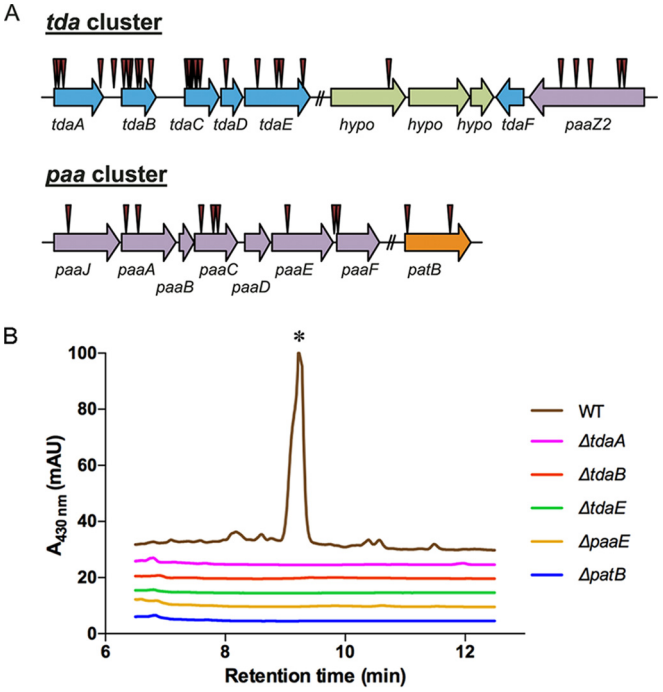

FIG 3 Biosynthetic genes required for roseobacticide production. (A) Transposon insertions into the *tda* and *paa* operons and the *patB* gene, which result in a roseobacticide-deficient phenotype. Black arrowheads indicate the sites of transposon insertion. (B) HPLC-MS results for the extracts of wt *P. inhibens* and selected mutant strains in the presence of sinapic acid. The starred peak in the wt trace represents roseobacticide B. All targeted knockout mutants failed to produce roseobacticide. The traces have been vertically offset for clarity.

mutants, giving a ~2-fold genome coverage. These mutants were then screened as described above. From our library, 85 mutants (~1%) exhibited a roseobacticide-deficient phenotype. The site of transposon insertion was determined using arbitrary PCR and resulted in 48 unique genes, whose disruption appeared to abolish roseobacticide production (Fig. 3A). These 48 genes grouped into several physiological pathways, including primary metabolism, DNA repair, substrate/product transport, phage-related genes, transcriptional regulators, sulfur insertion genes, the *paa* gene cluster (involved in aerobic degradation of phenylacetic acid), and the *tda* gene cluster (responsible for TDA biosynthesis). The possible biosynthetic genes are shown in Table 1, and all other genes are summarized in Table S1 in the supplemental material. To corroborate these results, a high-performance liquid chromatography-mass spectrometry (HPLC-MS) assay was conducted for each of the 85 Tn mutants, in which the presence of roseobacticide, if any, was quantitated. The results showed that 28 out of the 48 mutants were completely deficient in roseobacticide synthesis, while 18 mutants generated less than 5% of the roseobacticide generated by wt cultures. The remaining 2 mutants exhibited more than 5% roseobacticide compared with wt *P. inhibens* (Table 1; see also Table S1).

Of the category of genes detected, the *tda*, *paa*, and sulfur insertion genes represented the only potential biosynthetic genes, along with a number of genes of unknown function (Fig. 3A; Table 1) (28–32). The involvement of the *paa* cluster may have been predicted based on our recent results, in which we identified tropone hydrate, a product of the *paa* cluster, as a roseobacticide precursor (23). The involvement of the *tda* gene cluster, however, is surprising. The screen revealed that Tn insertion into numerous *tda* genes results in roseobacticide-deficient mutants, indicating that roseobacticide and TDA production share a number of biosynthetic enzymes. A number of genes of unknown function (Fig. 3A), notably a cluster of three such genes adjacent to the *tda* cluster, were uncovered in our screen as well. These did not display sequence similarities to any characterized genes in the known database and may be involved in the final stages of roseobacticide biosynthesis. The results above also indicate that enzymes encoded from at least three different genetic loci are necessary for roseobacticide production. As with TDA, a distinct coregulated biosynthetic gene cluster bearing all the necessary biosynthesis, transport, and resistance genes does not exist (28). Instead, the roseobacticide genes appear to be spread in several genetic loci.

An efficient method for creating targeted knockout mutants in *P. inhibens*. To further corroborate the transposon screening results described above and to test the idea that roseobacticide production requires biosynthetic genes from a number of genetic loci, we sought to generate site-directed gene inactivation mutants. Current strategies for mutagenizing *Roseobacter* utilize insertion of an antibiotic selection marker and growth on the requisite antibiotic (33). In our hands, this method frequently resulted in formation of merodiploid mutants. We addressed this shortcoming by creating a reliable mutagenesis procedure involving antibiotic selection followed by counterselection using the *pheS* toxic gene, which has previously been used for genetic manipulation of *Burkholderia* strains (34, 35). The product of *pheS*, an engineered tRNA synthetase, selectively incorporates *p*-chlorophenylalanine (*p*-Cl-Phe) into proteins. Cells that harbor this gene and are cultured in the presence of *p*-Cl-Phe incorporate the unnatural amino acid into the proteome, resulting in cell death.

TABLE 1 Putative biosynthetic genes required for roseobacticide production by *P. inhibens*[a]

Metabolic pathway and locus tag	Gene	% relative production[b]	Predicted function[c]
Phenylacetate catabolism			
PGA1_c04090	*paaJ*	0	β-Ketoadipyl-CoA thiolase
PGA1_c04080	*paaA*	0	Ring-1,2-phenylacetyl-CoA epoxidase[d]
PGA1_c04060	*paaC*	0	Ring-1,2-phenylacetyl-CoA epoxidase[d]
PGA1_c04040	*paaE*	0	Ring-1,2-phenylacetyl-CoA epoxidase[d]
Sulfur metabolism			
PGA1_c20760	*cysI*	4	Nitrite/sulfite reductase
PGA1_c00860	*patB*	0	Cystathionine β-lyase
TDA biosynthesis[e]			
PGA1_262p00980	*tdaA*	0	LysR transcriptional regulator
PGA1_262p00970	*tdaB*	0	β-Etherase
PGA1_262p00960	*tdaC*	0	Prephenate dehydratase
PGA1_262p00950	*tdaD*	0	Thioesterase
PGA1_262P00940	*tdaE*	0	Acyl-CoA dehydrogenase
PGA1_262p00800	*paaZ2*	0	Enoyl-CoA hydratase
PGA1_262p00840		0	PUF[f]

[a] See Table S1 in the supplemental material for a list of all other genes identified using the Tn mutagenesis screen.
[b] Production with each Tn mutant, relative to that of wt, determined using an HPLC-MS assay for direct detection of roseobacticide B.
[c] Predicted functions are based on protein homology to proteins in the IMG database.
[d] See reference 31.
[e] See reference 28.
[f] PUF, protein of unknown function.

The successful application of *pheS* as well as combination of an efficient selection and counterselection scheme enabled rapid and reliable production of marked and unmarked site-directed mutants in *P. inhibens*.

Implications for roseobacticide biosynthesis: the sulfur source. With a robust mutagenesis method in hand, we began to test the pathway for roseobacticide production. The genes implicated in sulfur insertion from our transposon data are PGA1_c20760, a putative sulfite reductase, and PGA1_c00860, a putative cystathionine-β-lyase (PatB) (Table 1). The latter gene, *patB*, was also implicated in sulfur insertion into TDA. Previously, cystathionine was proposed as the PatB substrate and the product homocysteine as the thiol donor for TDA production (6). More recently, based on early studies with *Escherichia coli* β-cystathionase (36), Brock et al. proposed cystine as the PatB substrate and *S*-thio-cysteine as the thiol donor (29). To further characterize the role of PatB, we generated a targeted *patB* mutant and observed that roseobacticide production was completely abolished in this strain (Fig. 3B). We then cloned and expressed *patB* as a NusA-His_6-tagged construct, as the corresponding His_6-PatB was insoluble, necessitating a solubility-enhancing domain. NusA-PatB co-purified with non-covalently bound PLP. Characterization of NusA-PatB showed that it did not react with L-Cys, glutathione, or cystathionine. Instead, it did react with cystine (Fig. 4A, compound 1), giving rise to two products, which we identified as *S*-thio-Cys (compound 2) and pyruvate, as predicted by Brock et al. (Fig. 4A) (29). *S*-Thio-Cys was identified by reaction with the thiol-reactive agent 5,5′-dithiobis-(2-nitrobenzoic acid) (DTNB) and detection of the product by HPLC-MS (see Fig. S2 in the supplemental material), while the presence of pyruvate was verified in a coupled lactate dehydrogenase assay (see Fig. S3 in the supplemental material). Based on the products of this reaction and knowledge of PLP-dependent transformations, a mechanism may be proposed for PatB (Fig. 4B) (37). PLP is bound by an active site Lys as an internal aldimine (compound 3). Formation of the external aldimine (compound 4) with cystine is followed by deprotonation of the now acidic α-proton, forming a resonance-stabilized carbanion at the α-carbon (compound 5). Subsequent β-elimination gives *S*-thio-Cys and an intermediate (compound 6). Aminolysis of this intermediate and tautomerization of the resulting product, followed by spontaneous imine hydrolysis, yield the products pyruvate and NH_3.

Combined with our previous findings, where we identified Cys as a sulfur precursor for roseobacticides (23), the results described above allowed us to propose a pathway for thiol group insertion (Fig. 4C). In this model, DMSP is converted to Cys, as previously reported (Fig. 4C, step *a*) (38). Formation of cystine provides the substrate for PatB (29), which generates *S*-thio-Cys (Fig. 4C, steps *b* and *c*). *S*-Thio-Cys is then used to insert thiol groups into TDA and roseobacticide (Fig. 4C, step *d*), a reaction proposed to be carried out by TdaB and TdaF in the case of TDA (29). While the details of this model need to be investigated, it does provide a direct pathway for incorporation of the DMSP-sulfur into roseobacticides via PatB. There are only a few biosynthetic pathways for insertion of thiols into small molecules (39). The experimental evidence thus far is consistent with a new biosynthetic mechanism for thiol group insertion in the production of roseobacticides. A similar conclusion was recently reached by Brock et al. for the biosynthesis of TDA (29).

Origins of the tropone. In *P. inhibens*, two pathways have been proposed for production of tropone: one of these involves the ring-expanding PaaN enzyme, while the second implicates the *paa* catabolon (Fig. 5A, *paaN* pathway versus *paa* catabolon pathway) (15, 30–32, 40). Our mutagenesis data implicated the *paa* catabolon in the production of roseobacticides (Table 1). These results were verified with a targeted *paaE* knockout mutant, which gave a roseobacticide-deficient phenotype (Fig. 3B). We propose that the *paa* catabolon provides the tropone precursor for roseobacticide synthesis.

Surprisingly, the *tda* locus was also implicated in our screen (Table 1). To verify this finding, we generated targeted knockout mutants for *tdaA*, a LysR-type transcriptional regulator that positively regulates TDA production in response to 3-OH–decanoyl-homoserine lactone (3-OH–C_{10}-HSL) (41, 42), *tdaB*, which encodes a putative sulfur insertion enzyme, *tdaC*, a putative prephenate dehydratase, *tdaD*, an acyl-CoA thioesterase, and *tdaE*, a putative acyl coenzyme A (CoA) dehydrogenase. With the exception of *tdaC*, we found all mutants to be deficient in roseobacticide biosynthesis, confirming the importance of these genes (Fig. 3B). The involvement of multiple *tda* genes in roseobacticide production suggests that the TDA and roseobacticide biosynthetic pathways share an intermediate, from which each pathway could diverge. Thus, elucidation of one pathway will necessitate understanding of the other.

The involvement of TdaA, TdaB, TdaD, and TdaE provides clues regarding roseobacticide synthesis. Brock et al. have proposed the most comprehensive model for TDA production (29). These enzymes are common to both pathways, whereas TdaC is

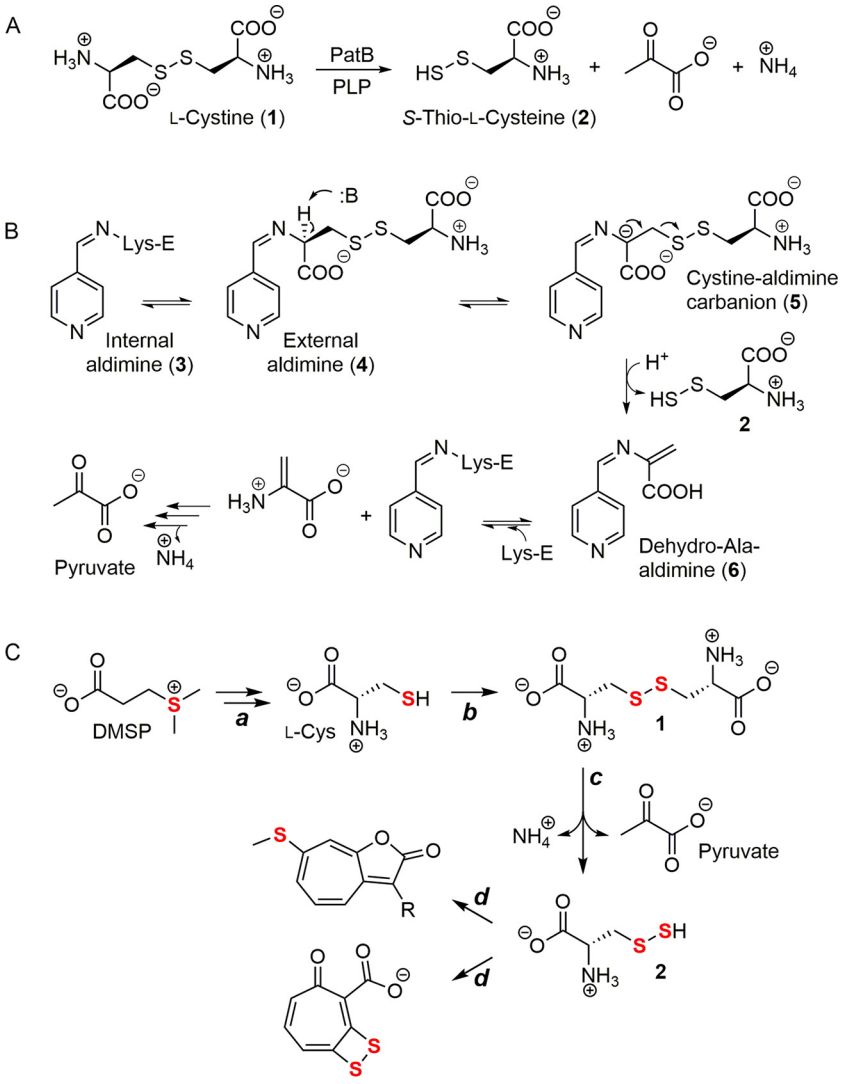

FIG 4 Involvement of PatB in roseobacticide biosynthesis. (A) Reaction catalyzed by PatB in the presence of cofactor PLP. (B) Proposed mechanism for PatB. See the text for further details. (C) Proposed pathway for incorporation of the DMSP sulfur into roseobacticides and TDA via PatB. Conversion of DMSP into Cys has been described (step *a*) (38). A cystine reductase may generate cystine from Cys (step *b*). PatB converts cystine to pyruvate and *S*-thio-Cys (step *c*). TdaB and TdaF may be involved in the insertion of S from *S*-thio-Cys into roseobacticides and TDA (step *d*) (29).

not required for either TDA or roseobacticide synthesis (28). In our current working model (Fig. 5A), which is based on the proposed pathway by Brock et al. (29), PaaABCDE generate epoxide 8 from phenylacetyl-CoA (compound 7), which is synthesized from phenylacetic acid by PaaK (30–32). Epoxide 8 is converted to oxepin-CoA (compound 9) by PaaG, which undergoes ring opening by PaaZ to give a linear product (compound 10). Two gene copies of a PaaZ derivative, which encode PaaZ1 and PaaZ2 with important E256Q and C295R mutations relative to PaaZ, then may catalyze formation of compound 11 (29). This compound may undergo dehydration, possibly spontaneously, to give intermediate compound 12, which could serve as a substrate for TdaB and TdaF. These enzymes could insert a thiol group by using *S*-thio-Cys, as previously proposed (29). The product of this reaction, compound 13, may be the last common intermediate in the production of TDA and roseobacticides. Insertion of a second thiol, followed by oxidation and CoA-thioester hydrolysis would furnish TDA, while reaction with the glyoxylyl-CoA (compound 14), as previously proposed (23), would lead to roseobacticides.

Consistent with the idea that the *tda* operon can synthesize two distinct compounds is the common substructure in TDA and roseobacticides involving the β-thiotropone moiety (Fig. 5B). That TDA and roseobacticide production share common intermediates and biosynthetic enzymes is an unexpected finding, one that has implications for the algal-bacterial symbiosis (see below).

Source of the aromatic side chain. Collectively, the data above provide insights into thiol insertion and the origin of the seven-membered ring in roseobacticides. A cluster of three hypothetical genes adjacent to the *tda* cluster were also implicated by our mutagenesis data (Fig. 3A; Table 1). HPLC-MS assays showed that Tn insertion into one of these genes abolished roseobacticide synthesis. Biochemical studies are necessary to investigate their possible role in incorporation of the amino acid portion of roseobacticides, as indicated by isotope feeding studies (23). Alternatively, it is

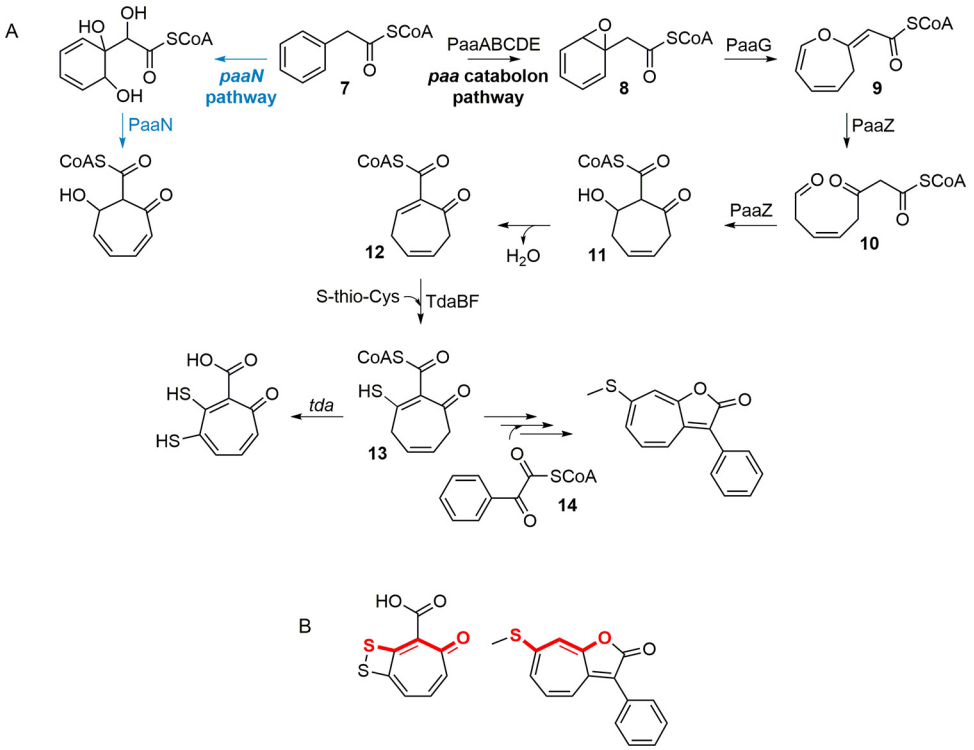

FIG 5 Working model for roseobacticide biosynthesis. (A) Two pathways can deliver the troponoid precursor for roseobacticides, the *paaN* pathway (blue arrows) or the *paa* catabolon pathway (black arrows). Our results are consistent with the involvement of the *paa* catabolon, which through the action of PaaABCDE delivers ring-1,2-epoxyphenylacetyl-CoA (compound 8) from phenylacetyl-CoA (compound 7), which is further elaborated into an oxepin-CoA (compound 9) via PaaG (30, 31). A bifunctional PaaZ could generate 3-hydroxy-5-cycloheptene-1-one-2-formyl-CoA (compound 11) via 3-oxo-5,6-dehydrosuberyl-CoA semialdehyde (compound 10), which through possibly spontaneous loss of water would furnish intermediate compound 12 (2,5-cycloheptadiene-1-one-2-formyl-CoA). This may serve as a substrate for thiol insertion putatively via TdaB and TdaF to give the β-thiotropone analog (compound 13) (29), possibly the last common intermediate in the TDA and roseobacticides pathways. Addition of another thiol, oxidation, and hydrolysis of the CoA-thioester would give the reduced form of TDA, while reaction with a glyoxylyl-CoA (compound 14) and further modifications would give roseobacticides. The orders of these latter steps are not known in either pathway. (B) Highlighted is the β-thiotropone substructure within both TDA and roseobacticide B. This shared moiety might explain the common biosynthetic origins for these structurally and functionally distinct molecules.

possible that our screen did not capture the genes responsible for this aspect of roseobacticide production and additional studies may be necessary to uncover all the genes required for roseobacticide synthesis.

Regulation of roseobacticide biosynthesis. The transposon screen provided two clues regarding the regulation of roseobacticide synthesis. First, the involvement of the *tda* cluster, which is regulated by the autoinducer 3-OH−C_{10}-HSL (42), suggests that roseobacticide biosynthesis may also be QS regulated. Second, two transcriptional regulators were found in the transposon screen that resulted in a roseobacticide-deficient phenotype. We first sought to corroborate these result and eliminate the possibility of polar effects resulting from transposon insertion. Both transcriptional regulator mutants retained the ability to generate roseobacticide, inconsistent with a role in its synthesis. To examine possible QS regulation, we generated a homoserine lactone synthase mutant strain, strain Δ*pgaI*, which lacks the ability to produce 3-OH–C_{10}-HSL, the signal that induces the *tda* cluster (42). HPLC-MS assays showed that this mutant also lost the ability to synthesize roseobacticides (Fig. 6). However, when purified 3-OH–C_{10}-HSL was added to the Δ*pgaI* strain cultures, or when the mutant was cocultured with a Δ*tdaA* strain, roseobacticide synthesis was restored (Fig. 6). Accordingly, one strain, the Δ*tdaA* strain, secretes the 3-OH−C_{10}-HSL signal, while the Δ*pgaI* strain can generate roseobacticides. Further, examination of the time course of roseobacticide production showed that it is not produced at low cell densities, but rather in late stationary phase. Addition of the QS signal 3-OH−C_{10}-HSL led to an earlier induction of roseobacticide biosynthesis (see Fig. S4 in the supplemental material). Col-

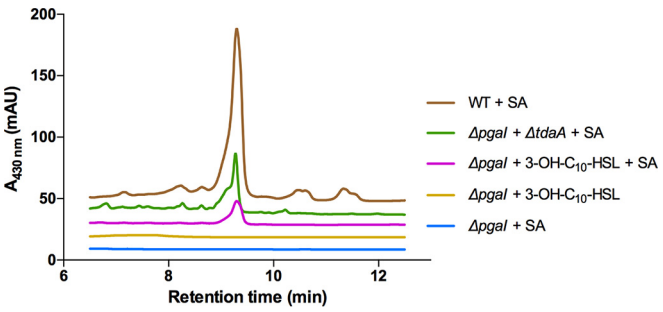

FIG 6 Roseobacticide biosynthesis is regulated by quorum sensing via 3-OH–C_{10}-HSL. HPLC-MS profiles are shown for extracts of wt *P. inhibens* and selected mutant strains in the presence of sinapic acid (SA). The peak in the wt trace corresponds to roseobacticide B. The Δ*tdaA* and Δ*pgaI* strains individually failed to produce roseobacticides, while a coculture of these mutant strains, or a Δ*pgaI* strain culture supplemented with 3-OH–C_{10}-HSL, generated roseobacticides. The traces have been vertically offset for clarity.

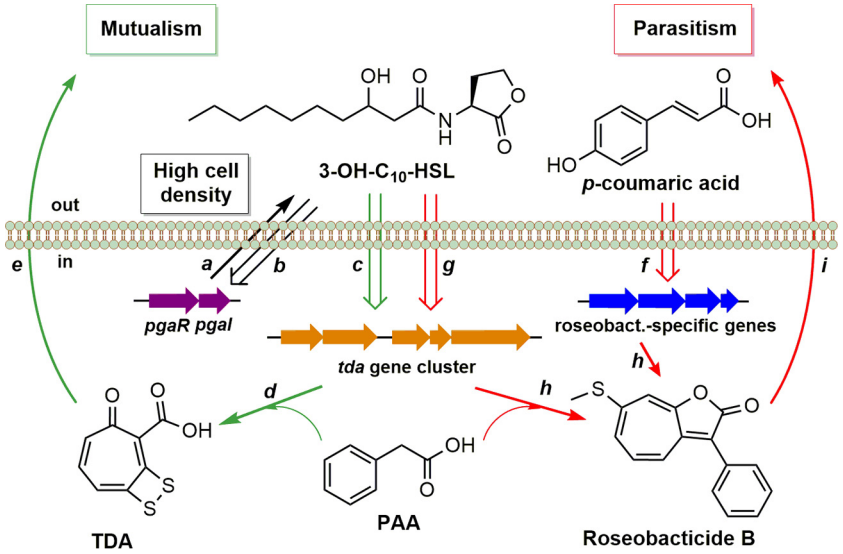

FIG 7 Preliminary regulatory model for roseobacticide production. Single arrows indicate biosynthetic processes or small-molecule secretion, while double arrows connote induction of gene expression. Growth in the mutualistic phase at high cell densities leads to production of 3-OH–C_{10}-HSL via PgaI, a homoserine lactone synthase (step *a*) (42). At threshold concentrations, this signal positively regulates *pgaR/pgaI* gene expression (step *b*) as well as expression of *tdaA* (step *c*), which induces the *tda* cluster and leads to production of TDA (42), a molecule that we propose protects the algal host (steps *d* and *e*) (2). However, in the parasitic phase, algal *p*-coumaric acid, or other phenylpropanoids, such as sinapic acid (2, 11), induce roseobacticide-specific genes (step *f*), which in conjunction with the *tda* operon give rise to roseobacticide (steps *g* and *h*), a potent toxin that kills the algal host (step *i*). Note that pCA serves as a precursor and an inducer for some roseobacticides, such as roseobacticide A (see Fig. 1) (23), while for other analogs, such as roseobacticide B or C, it acts only as an inducer.

lectively, these results demonstrate that roseobacticide production is regulated by QS via 3-OH−C_{10}-HSL and have important implications for the algal-bacterial symbiosis, notably, the pathogenic phase of this interaction.

A preliminary regulatory framework for roseobacticide biosynthesis may be conceived. Under normal, mutualistic conditions, production and detection of 3-OH−C_{10}-HSL at high bacterial cell densities leads to synthesis of TDA, which has been proposed to protect the algal host from pathogenic bacteria (Fig. 7). In this mode of interaction, roseobacticide synthesis is turned off. When the host senesces, it releases pCA, which is presumably detected at the cell surface by *P. inhibens*. The combination of pCA and 3-OH−C_{10}-HSL then leads to production of TDA and roseobacticides (Fig. 7). To ensure tight regulation of algaecide production and firm control over a proposed lifestyle switch from mutualism to parasitism, roseobacticide biosynthesis necessitates the presence of two signals, algal pCA and bacterial 3-OH−C_{10}-HSL.

Conclusions. In response to algal phenylpropanoids, *P. inhibens* synthesizes roseobacticides, which has been proposed to initiate a mutualist-to-parasite switch in its symbiosis with an algal host. Much like other critical cellular processes, such as sporulation or virulence factor production, this lifestyle switch is tightly regulated (43–47). Herein, we begin to delineate the components of this regulatory process. Not only is the algal metabolite pCA or a similar inducer, such as sinapic acid, necessary for roseobacticide production, but this process is also under QS control and requires the autoinducer 3-OH−C_{10}-HSL. Roseobacticides join a long list of other toxins that are activated by QS, but in this case, QS is necessary but not sufficient. While our findings have identified a key feature in the regulatory cascade of roseobacticide synthesis, this picture is far from complete and will receive further attention in the future.

We further defined the molecular underpinnings of the rapid switch-like behavior from mutualism to parasitism by *P. inhibens*. TDA and roseobacticides are largely generated by the same biosynthetic enzymes. This enables *P. inhibens* to merely divert an already active biosynthetic pathway toward the synthesis of roseobacticides, rather than inducing a new pathway. By intertwining roseobacticide and TDA biosyntheses, the bacterium preserves precious nutrients and precursors, allowing it a rapid lifestyle switch in response to algal senescence. In addition, the production of two distinct metabolites from largely one set of genes amplifies the secondary metabolic potential of *P. inhibens*.

Our studies set the stage for the characterization of a number of enzymes involved in production of both rare troponoid compounds. Initial forays in this regard have begun to delineate a pathway for sulfur and phenylacetic acid insertion into the roseobacticides. While the biochemical steps still need to be elucidated, the evidence thus far suggests that new enzymatic transformations remain to be discovered in the production of these troponoids, especially with respect to tropolactone formation and the insertion of thiol groups.

MATERIALS AND METHODS

Bacterial strains and growth conditions. *P. inhibens* DSM 17395 was used throughout this study (48). It was routinely cultured in marine broth (MB; Difco) or in half-strength YTSS medium (referred to as ½YTSS, containing, per liter, 20 g Sigma sea salt, 2 g yeast extract, 1.25 g tryptone) (2).

DNA manipulations. Genomic DNA was isolated using the Wizard gDNA isolation kit (Promega). Transposon mutagenesis was carried out with the EZ-Tn*5* transposome kit (Epicentre) (49). PCRs were performed with *Taq* DNA polymerase (NEB) for arbitrary PCR or with Q5 DNA polymerase (NEB) for cloning and genetic manipulations. T4 DNA ligase (NEB) was used for ligation reactions. *E. coli* DH5α cells (NEB) and

BL21(DE3) cells (NEB) were used for cloning and expression, respectively.

Transposon mutagenesis. Competent *P. inhibens* cells were created via the procedure previously described, with minor modifications (42). Briefly, a 5-ml overnight culture of *P. inhibens* in marine broth was grown in a 14-ml sterile culture tube at 30°C and 250 rpm. It was then diluted 50-fold into 175 ml of marine broth in a 1-liter Erlenmeyer flask. After 7 to 8 h, an OD_{600} of ~0.5 was reached, at which point the flask was incubated in ice-water for 15 min and gently swirled several times during that period. Cells were then pelleted by centrifugation (4°C, 2,500 × *g*, 8 min) and resuspended in 120 ml of ice-cold sterile 10% (vol/vol) glycerol. This process of centrifugation and resuspension in 10% glycerol was repeated four more times. After the last spin cycle, the cells were resuspended in 0.7 ml of 10% glycerol, distributed in 40-μl aliquots, and flash-frozen in liquid N_2. To create *P. inhibens* mutants strains, an aliquot was thawed on ice, 1 μl of the EZ-Tn5 transposome mix was added, and the mixture was transferred to a 1-mm electroporation cuvette. The mixture was electroporated at 1,375 V for 5 ms, then immediately returned to ice, supplemented with 1 ml marine broth, and transferred to a 14-ml sterile culture tube. The cells were cultured at 250 rpm at 30°C for 4 h and then plated on ½YTSS medium containing 50 μg/ml kanamycin.

High-throughput fluorescence assay for roseobacticide production. After transposon mutagenesis, ~8,000 colonies were arrayed into 96-well plates containing ½YTSS supplemented with 50 μg/ml kanamycin. The cultures were grown at 250 rpm and 30°C overnight, and supplemented with a final concentration of 15% glycerol and kept at −80°C. For each round of assay, clear-bottom, black-walled 96-well assay plates were filled with 150 μl of ½YTSS supplemented with 1 mM sinapic acid by using a MultiFlo microplate dispenser (BioTek). The assay plate was inoculated with ~3 μl of the library plate using a CyBi-well automated liquid transfer system (CyBio). The plates were sealed with a membrane and grown at 30°C and 250 rpm for 3 days. After 3 days, emission spectra were recorded with an H1MF plate reader (BioTek) by excitation at 430 nm and emission between 450 and 700 nm.

Creating targeted knockout mutants in *P. inhibens*. Gene deletion mutants were created with a new procedure using gentamicin positive selection and a *pheS* counterselection cycle (see Table S2 in the supplemental material). The *pheS* gene was cloned from vector pEX18Km-*pheS* (35) using the primers 5′-AGCACTGAGCTCCTTGTCTGTAAGCGGA TGCCGGG-3′ and 5′-AGCAATTCTAGACCGGC GTAACAGTACTGA GGGC-3′ into pBluescript KS(−), generating parent plasmid pRW01. For each deletion, a knockout plasmid was constructed by inserting a knockout cassette, consisting of a gentamicin resistance gene cloned from pEX18Gm-*pheS* (35) flanked by a 1-kb DNA sequence upstream and downstream of the gene to be deleted, into the parent plasmid pRW01. At least 500 ng of the knockout plasmid was transformed into *P. inhibens* by electroporation as described above. Desired cells were selected on MB agar containing 25 μg/ml gentamicin. These were subjected to counterselection on ½YTSS agar containing 0.1% p-Cl-phenylalanine. Mutants were verified by colony PCR and DNA sequencing of the amplified fragment.

HPLC-MS detection of roseobacticides. Roseobacticide production was routinely assayed by an HPLC-MS procedure. A 5-ml overnight culture of the desired mutant or wt strain was cultured in a 14-ml sterile culture tube in ½YTSS. Tn5 mutated strain cultures contained kanamycin (50 μg/ml). The overnight cultures were grown at 30°C and 250 rpm. The next day, each overnight culture was diluted into 15 ml of ½YTSS supplemented with 1 mM sinapic acid in a 125-ml Erlenmeyer flask. The cultures were grown at 30°C and 160 rpm for 3 days. They were then extracted with a 1:1 (vol/vol) of ethyl acetate. The organic layer was dried *in vacuo*, resuspended in ~0.5 ml methanol, and analyzed on an Agilent HPLC-MS instrument consisting of a liquid autosampler, a 1260 Infinity series HPLC system coupled to a photodiode array detector and a 6120 series electrospray ionization (ESI) mass spectrometer. A Phenomenex Luna C_{18} column (5 μm, 4.6 by 100 mm) was used with a flow rate of 0.6 ml/min and a gradient of 40 to 100% acetonitrile in H_2O over 20 min.

Cloning, expression, and purification of PatB. *patB* was amplified from *P. inhibens* gDNA by using primers 5′-CGCTCGGGATCCATGAA TTTTGACAAGATCATTGATCGCCGG-3′ and 5′-CGCTCGGGATCC ATGAATTTTGACAAGATCATTGATCGCCGG-3′ and then cloning into vector pSJ7, which contains a pBR322 origin of replication and an N-terminal NusA purification tag. PatB was expressed in *E. coli* BL21(DE3) cells in LB. Large-scale cultures (four 1-liter LB cultures in 4-liter Erlenmeyer flasks) were grown at 37°C to an OD_{600} of ~0.6 and then induced with 0.1 mM isopropyl-β-D-thiogalactopyranoside. The temperature was lowered to 18°C, and expression was carried out for 18 h. At that point, the cells were pelleted by centrifugation, flash-frozen in liquid N_2, and stored at −80°C. Protein purification was carried out at 4°C. Each gram of cell pellet was resuspended in 5 ml of buffer A (20 mM Tris-HCl [pH 7.4], 250 mM NaCl, 5 mM imidazole, 5% glycerol, and 0.1% Triton) and supplied with a protease inhibitor cocktail (Sigma). The homogenized cells were lysed by sonication using a Branson ultrasonic cell disrupter operating at 65% power with 15 iterations of 10-s on/20-s off cycles. Cell debris was removed by centrifugation, and the crude extract was passed over an Ni^{2+}-nitrilotriacetic acid column (5 ml, 4-cm length, 1.25-cm diameter; Clontech). NusA-PatB was eluted with a step gradient of buffer A containing 50 mM, 100 mM, 200 mM, and 500 mM imidazole. NusA-PatB was detected in the last two fractions by SDS-PAGE. The protein was exchanged into storage buffer (50 mM Tris-HCl [pH 7.4], 500 mM NaCl, 0.2 mM EDTA, and 5% glycerol) on a Sephadex G-25 column (30 ml, 25-cm length, 1.25-cm diameter) and stored at a concentration of 36.3 mg/ml at −80°C. An extinction coefficient of 98,945 M^{-1} cm^{-1} was used to determine NusA-PatB concentrations.

Characterization of PatB. PatB activity was assayed in a continuous spectrophotometric assay using the thiol-reactive agent DTNB. The reaction mixture contained (in a final volume of 300 μl) 100 mM Tris-HCl (pH 9.0), 0.2 mM DTNB, 0.1 mM PLP, 2 mM substrate (L-glutathione, L-cystathionine, or L-cystine), and 10 μM purified NusA-PatB. The increase in absorbance at 412 nm was measured at an interval of 0.02 min for 5 min at room temperature. A molar extinction coefficient of 13,400 M^{-1} cm^{-1} for the aryl mercaptide was used to calculate the amount of product formed. To verify formation of pyruvate as a product in the NusA-PatB reaction, a coupled lactate dehydrogenase (LDH) assay was carried out. The reaction mixture contained, in a final volume of 300 μl, 100 mM Tris-HCl (pH 9.0), 0.1 mM PLP, 2 mM L-cystine, 0.2 mM NADH, 10 μM purified NusA-PatB, and 6 U of LDH. The consumption of NADH was measured at 340 nm at an interval of 0.02 min for 5 min at room temperature.

SUPPLEMENTAL MATERIAL

Supplemental material for this article may be found at http://mbio.asm.org/lookup/suppl/doi:10.1128/mBio.02118-15/-/DCSupplemental.

Figure S1, EPS file, 1.5 MB.
Figure S2, EPS file, 1.7 MB.
Figure S3, EPS file, 1.3 MB.
Figure S4, EPS file, 1.2 MB.
Table S1, DOCX file, 0.02 MB.
Table S2, DOCX file, 0.02 MB.

ACKNOWLEDGMENTS

We thank Hera Vlamakis and Roberto Kolter for valuable advice in creating gene deletions and transposon insertions in *P. inhibens*.

We gratefully acknowledge the National Institutes of Health (grant GM098299 to M.R.S.) and the Pew Biomedical Scholars Program (to M.R.S.) for support of this work.

REFERENCES

1. **Weber T, Blin K, Duddela S, Krug D, Kim HU, Bruccoleri R, Lee SY, Fischbach MA, Müller R, Wohlleben W, Breitling R, Takano E, Medema MH.** 2015. antiSMASH 3.0—a comprehensive resource for the genome mining of biosynthetic gene clusters. Nucleic Acids Res **43:** W237–W243. http://dx.doi.org/10.1093/nar/gkv437.

2. **Seyedsayamdost MR, Case RJ, Kolter R, Clardy J.** 2011. The Jekyll-and-Hyde chemistry of *Phaeobacter gallaeciensis*. Nat Chem **3:**331–335. http://dx.doi.org/10.1038/nchem.1002.
3. **Wagner-Döbler I, Biebl H.** 2006. Environmental biology of the marine Roseobacter lineage. Annu Rev Microbiol **60:**255–280. http://dx.doi.org/10.1146/annurev.micro.60.080805.142115.
4. **Buchan A, González JM, Moran MA.** 2005. Overview of the marine Roseobacter lineage. Appl Environ Microbiol **71:**5665–5677. http://dx.doi.org/10.1128/AEM.71.10.5665-5677.2005.
5. **Geng H, Belas R.** 2010. Molecular mechanisms underlying Roseobacter-phytoplankton symbioses. Curr Opin Biotechnol **21:**332–338. http://dx.doi.org/10.1016/j.copbio.2010.03.013.
6. **Thole S, Kalhoefer D, Voget S, Berger M, Engelhardt T, Liesegang H, Wollherr A, Kjelleberg S, Daniel R, Simon M, Thomas T, Brinkhoff T.** 2012. *Phaeobacter gallaeciensis* genomes from globally opposite locations reveal high similarity of adaptation to surface life. ISME J **6:**2229–2244. http://dx.doi.org/10.1038/ismej.2012.62.
7. **Slightom RN, Buchan A.** 2009. Surface colonization by marine roseobacters: integrating genotype and phenotype. Appl Environ Microbiol **75:**6027–6037. http://dx.doi.org/10.1128/AEM.01508-09.
8. **Rao D, Webb JS, Holmström C, Case R, Low A, Steinberg P, Kjelleberg S.** 2007. Low densities of epiphytic bacteria from the marine alga *Ulva australis* inhibit settlement of fouling organisms. Appl Environ Microbiol **73:**7844–7852. http://dx.doi.org/10.1128/AEM.01543-07.
9. **Matsuo Y, Imagawa H, Nishizawa M, Shizuri Y.** 2005. Isolation of an algal morphogenesis inducer from a marine bacterium. Science **307:**1598. http://dx.doi.org/10.1126/science.1105486.
10. **Keshtacher-Liebso E, Hadar Y, Chen Y.** 1995. Oligotrophic bacteria enhance algal growth under iron-deficient conditions. Appl Environ Microbiol **61:**2439–2441.
11. **Seyedsayamdost MR, Carr G, Kolter R, Clardy J.** 2011. Roseobacticides: small molecule modulators of an algal-bacterial symbiosis. J Am Chem Soc **133:**18343–18349. http://dx.doi.org/10.1021/ja207172s.
12. **Seymour JR, Simó R, Ahmed T, Stocker R.** 2010. Chemoattraction to dimethylsulfoniopropionate throughout the marine microbial food web. Science **329:**342–345. http://dx.doi.org/10.1126/science.1188418.
13. **González JM, Kiene RP, Moran MA.** 1999. Transformation of sulfur compounds by an abundant lineage of marine bacteria in the alpha-subclass of the class Proteobacteria. Appl Environ Microbiol **65:**3810–3819.
14. **Miller TR, Hnilicka K, Dziedzic A, Desplats P, Belas R.** 2004. Chemotaxis of *Silicibacter* sp. strain TM1040 toward dinoflagellate products. Appl Environ Microbiol **70:**4692–4701. http://dx.doi.org/10.1128/AEM.70.8.4692-4701.2004.
15. **Thiel V, Brinkhoff T, Dickschat JS, Wickel S, Grunenberg J, Wagner-Döbler I, Simon M, Schulz S.** 2010. Identification and biosynthesis of tropone derivatives and sulfur volatiles produced by bacteria of the marine Roseobacter clade. Org Biomol Chem **8:**234–246. http://dx.doi.org/10.1039/b909133e.
16. **Ashen JB, Cohen JD, Goff LJ.** 1999. GC-SIM-MS detection and quantification of free indole-3-acetic acid in bacterial galls on the marine alga *Prionitis lanceolata* (Rhodophyta). J Phycol **35:**493–500. http://dx.doi.org/10.1046/j.1529-8817.1999.3530493.x.
17. **D'Alvise PW, Lillebø S, Prol-Garcia MJ, Wergeland HI, Nielsen KF, Bergh Ø, Gram L.** 2012. *Phaeobacter gallaeciensis* reduces *Vibrio anguillarum* in cultures of microalgae and rotifers, and prevents vibriosis in cod larvae. PLoS One **7:**e43996. http://dx.doi.org/10.1371/journal.pone.0043996.
18. **D'Alvise PW, Melchiorsen J, Porsby CH, Nielsen KF, Gram L.** 2010. Inactivation of *Vibrio anguillarum* by attached and planktonic Roseobacter cells. Appl Environ Microbiol **76:**2366–2370. http://dx.doi.org/10.1128/AEM.02717-09.
19. **Planas M, Pérez-Lorenzo M, Hjelm M, Gram L, Uglenes Fiksdal I, Bergh Ø, Pintado J.** 2006. Probiotic effect in vivo of Roseobacter strain 27-4 against *Vibrio* (*Listonella*) *anguillarum* infections in turbot (*Scophthalmus maximus* L.) larvae. Aquaculture **255:**323–333. http://dx.doi.org/10.1016/j.aquaculture.2005.11.039.
20. **González JM, Simó R, Massana R, Covert JS, Casamayor EO, Pedrós-Alió C, Moran MA.** 2000. Bacterial community structure associated with a dimethylsulfoniopropionate-producing North Atlantic algal bloom. Appl Environ Microbiol **66:**4237–4246. http://dx.doi.org/10.1128/AEM.66.10.4237-4246.2000.
21. **Lamy D, Obernosterer I, Laghdass M, Artigas F, Breton E, Grattepanche J, Lecuyer E, Degros N, Lebaron P, Christaki U.** 2009. Temporal changes of major bacterial groups and bacterial heterotrophic activity during a *Phaeocystis globosa* bloom in the eastern English Channel. Aquat Microb Ecol **58:**95–107. http://dx.doi.org/10.3354/ame01359.
22. **Wang H, Tomasch J, Jarek M, Wagner-Döbler I.** 2014. A dual-species co-cultivation system to study the interactions between Roseobacters and dinoflagellates. Front Microbiol **5:**311. http://dx.doi.org/10.3389/fmicb.2014.00311.
23. **Seyedsayamdost MR, Wang R, Kolter R, Clardy J.** 2014. Hybrid biosynthesis of roseobacticides from algal and bacterial precursor molecules. J Am Chem Soc **136:**15150–15153. http://dx.doi.org/10.1021/ja508782y.
24. **Kintaka K, Ono H, Tsubotani S, Harada S, Okazaki H.** 1984. Thiotropocin, a new sulfur-containing 7-membered ring antibiotic produced by a *Pseudomonas* sp. J Antibiot **37:**1294–1300. http://dx.doi.org/10.7164/antibiotics.37.1294.
25. **Bruhn JB, Nielsen KF, Hjelm M, Hansen M, Bresciani J, Schulz S, Gram L.** 2005. Ecology, inhibitory activity, and morphogenesis of a marine antagonistic bacterium belonging to the *Roseobacter clade*. Appl Environ Microbiol **71:**7263–7270. http://dx.doi.org/10.1128/AEM.71.11.7263-7270.2005.
26. **Greer EM, Aebisher D, Greer A, Bentley R.** 2008. Computational studies of the tropone natural products, thiotropocin, tropodithietic acid, and troposulfenin. Significance of thiocarbonyl-enol tautomerism. J Org Chem **73:**280–283. http://dx.doi.org/10.1021/jo7018416.
27. **Bentley R.** 2008. A fresh look at natural tropolonoids. Nat Prod Rep **25:**118–138. http://dx.doi.org/10.1039/b711474e.
28. **Geng H, Bruhn JB, Nielsen KF, Gram L, Belas R.** 2008. Genetic dissection of tropodithietic acid biosynthesis by marine roseobacters. Appl Environ Microbiol **74:**1535–1545. http://dx.doi.org/10.1128/AEM.02339-07.
29. **Brock NL, Nikolay A, Dickschat JS.** 2014. Biosynthesis of the antibiotic tropodithietic acid by the marine bacterium *Phaeobacter inhibens*. Chem Commun (Camb) **50:**5487–5489. http://dx.doi.org/10.1039/c4cc01924e.
30. **Teufel R, Gantert C, Voss M, Eisenreich W, Haehnel W, Fuchs G.** 2011. Studies on the mechanism of ring hydrolysis in phenylacetate degradation. J Biol Chem **286:**11021–11034. http://dx.doi.org/10.1074/jbc.M110.196667.
31. **Teufel R, Friedrich T, Fuchs G.** 2012. An oxygenase that forms and deoxygenates toxic epoxide. Nature **483:**359–362. http://dx.doi.org/10.1038/nature10862.
32. **Berger M, Brock NL, Liesegang H, Dogs M, Preuth I, Simon M, Dickschat JS, Brinkhoff T.** 2012. Genetic analysis of the upper phenylacetate catabolic pathway in the production of tropodithietic acid by *Phaeobacter gallaeciensis*. Appl Environ Microbiol **78:**3539–3551. http://dx.doi.org/10.1128/AEM.07657-11.
33. **Piekarski T, Buchholz I, Drepper T, Schobert M, Wagner-Doebler I, Tielen P, Jahn D.** 2009. Genetic tools for the investigation of Roseobacter clade bacteria. BMC Microbiol **9:**265. http://dx.doi.org/10.1186/1471-2180-9-265.
34. **Reyrat JM, Pelicic V, Gicquel G, Rappuoli R.** 1998. Counterselectable markers: untapped tools for bacterial genetics and pathogenesis. Infect Immun **66:**4011–4017.
35. **Barrett AR, Kang Y, Inamasu KS, Son MS, Vukovich JM, Hoang TT.** 2008. Genetic tools for allelic replacement in *Burkholderia* species. Appl Environ Microbiol **74:**4498–4508. http://dx.doi.org/10.1128/AEM.00531-08.
36. **Uren JR.** 1987. Cystathionine β-lyase from *Escherichia coli*. Methods Enzymol **17:**483–486.
37. **Eliot AC, Kirsch JF.** 2004. Pyridoxal phosphate enzymes: mechanistic, structural, and evolutionary considerations. Annu Rev Biochem **73:**383–415. http://dx.doi.org/10.1146/annurev.biochem.73.011303.074021.
38. **Kiene RP, Linn LJ, González J, Moran MA, Bruton JA.** 1999. Dimethylsulfoniopropionate and methanethiol are important precursors of methionine and protein-sulfur in marine bacterioplankton. Appl Environ Microbiol **65:**4549–4558.
39. **Mueller EG.** 2006. Trafficking in persulfides: delivering sulfur in biosynthetic pathways. Nat Chem Biol **2:**185–194. http://dx.doi.org/10.1038/nchembio779.
40. **Cane DE, Wu Z, Van Epp JE.** 1992. Thiotropocin biosynthesis. Shikimate origin of a sulfur-containing tropolone derivative. J Am Chem Soc **114:**8479–8483. http://dx.doi.org/10.1021/ja00048a019.
41. **Geng H, Belas R.** 2011. Tda A regulates tropodithietic acid synthesis by binding to the tdaC promoter region. J Bacteriol **193:**4002–4005. http://dx.doi.org/10.1128/JB.00323-11.
42. **Berger M, Neumann A, Schulz S, Simon M, Brinkhoff T.** 2011. Tropo-

dithietic acid production in Phaeobacter gallaeciensis is regulated by N-acyl homoserine lactone-mediated quorum sensing. J Bacteriol **193:** 6576–6585. http://dx.doi.org/10.1128/JB.05818-11.

43. **Fuqua C, Parsek MR, Greenberg EP**. 2001. Regulation of gene expression by cell-to-cell communication: acyl-homoserine lactone quorum sensing. Annu Rev Genet **35:**439–468. http://dx.doi.org/10.1146/annurev.genet.35.102401.090913.
44. **Fuqua C, Greenberg EP**. 2002. Listening in on bacteria: acyl-homoserine lactone signalling. Nat Rev Mol Cell Biol **3:**685–695. http://dx.doi.org/10.1038/nrm907.
45. **Waters CM, Bassler BL**. 2005. Quorum sensing: cell-to-cell communication in bacteria. Annu Rev Cell Dev Biol **21:**319–346. http://dx.doi.org/10.1146/annurev.cellbio.21.012704.131001.
46. **Bassler BL, Losick R**. 2006. Bacterially speaking. Cell **125:**237–246. http://dx.doi.org/10.1016/j.cell.2006.04.001.
47. **Straight PD, Kolter R**. 2009. Interspecies chemical communication in bacterial development. Annu Rev Microbiol **63:**99–118. http://dx.doi.org/10.1146/annurev.micro.091208.073248.
48. **Martens T, Heidorn T, Pukall R, Simon M, Tindall BJ, Brinkhoff T**. 2006. Reclassification of Roseobacter gallaeciensis Ruiz-Ponte et al. 1998 as Phaeobacter gallaeciensis gen. nov., comb. nov., description of Phaeobacter inhibens sp. nov., reclassification of Ruegeria algicola (Lafay et al. 1995) Uchino et al. 1999 as Marinovum algicola gen. nov., comb. nov., and emended descriptions of the genera Roseobacter, Ruegeria and Leisingera. Int J Syst Evol Microbiol **56:**1293–1304. http://dx.doi.org/10.1099/ijs.0.63724-0.
49. **Goryshin IY, Jendrisak J, Hoffman LM, Meis R, Reznikoff WS**. 2000. Insertional transposon mutagenesis by electroporation of released Tn5 transposition complexes. Nat Biotechnol **18:**97–100. http://dx.doi.org/10.1038/72017.